

Poster session 2: Application for Biofabrication – in vitro models

P2.1

Silk-Fibroin-Cryogels as 3D culture model system in the field of cancer research

Anne Bäcker, Thomas Sollich, Paul Abaffy, Olga Fominov, Angelica Cecilia, Friederike Jana Gruhl
KIT, Eggenstein-Leopoldshafen, Germany

Introduction: In many cases the scaffolds are often tailor-made and allow no significant structural or chemical change [1]. The aim of this study was to synthesize cryogel matrices based on natural polymers whereas the blend mainly consists of the silkworm protein fibroin. Both fibroin types from *Bombyx mori* and *Antheraea pernyi* are co-polymerized with a number of different materials such as collagen, gelatin, chitosan, which are currently being employed for variety applications. Interesting changes in cell growth behavior and a new understanding in the selection of synthesis parameter for the design of 3D polymeric matrices are discussed [2].

Materials & Methods: The specific characteristic features of the silk-fibroin (SF)-cryogels were investigated by several qualitative and quantitative methods. These include studies to the material elasticity by unconfined compression test and total porosity (including pore distribution, pore size and shape) by scanning electron microscope, mercury porosimetry, x-ray microtomography as well as the measurement of swelling kinetics. Furthermore, the proliferation behaviour of the epithelial prostate cancer cell line LnCaP was examined by gathering the growth rate over 21 days. Additionally, specific staining methods (HE-staining, Immunofluorescence) help to investigate the size and distribution of the formed spheroids and localisation of the androgen receptor.

Results: Recent results demonstrate that the different SF-cryogel compositions show a high interconnected pore system with various pore sizes as well as swelling kinetics and elasticity. The cell viability and proliferation as a function of time are indicative of the cellular compatibility and suitability for numerous applications. The synthesized matrices were characterized by various standard methods to evaluate the effect of component concentration, crosslinking and freezing-time on the cryogel properties as well as the cultured cell line.

Discussion: The SF and different natural components were blended in varying volume ratios and 3D scaffolds were prepared. These compositions allow the formation of microstructures that enhanced cell adherence and ingrowth. The folded pore structure provides the LnCaP cells the required pore surface and volume to form cell spheroids.

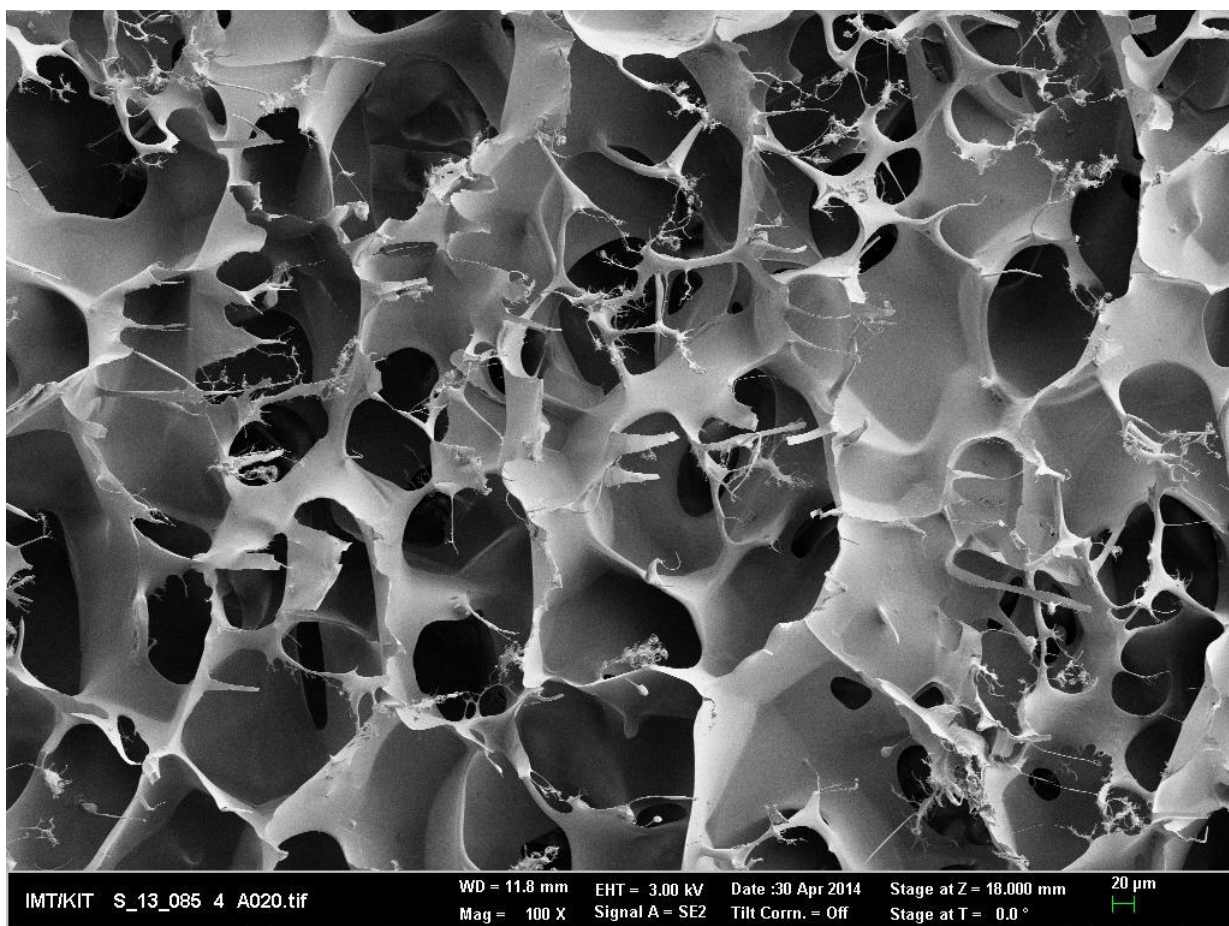
References:

- [1] Bhardwaj et al. 2011
- [2] Baecker et al. 2014

Acknowledgements:

The authors would like to acknowledge the Ministry of Rural Affairs and Consumer Protection of Baden-Württemberg for the foundation of the project.





Scanning electron microscope (SEM) image of the silk-fibroin blend of chitosan and B.mori.

P2.2

Biofabrication of perfusable liver constructs

Monique Schuddeboom, Ferry Melchels, Baukje Schotanus, Jos Malda, Bart Spee
Utrecht University, Utrecht, Netherlands

Current in vitro systems do not allow an accurate prediction of drug-induced liver injury (DILI). This is one of the main reasons why DILI still occurs in clinical phases of drug development or even post-marketing which makes it a serious health concern. Our approach is to develop a biofabricated 3D liver construct that can be cultured in a custom designed bioreactor system. As such these perfusable constructs will better mimic the liver compared to a 2D hepatocyte culture. To achieve this biofabrication techniques were employed with liver cell lines and gelMA hydrogel in a 3D bioprinter.

Methods: As a source of hepatocytes adult stem cells of the liver termed liver organoids or a hepatic cell line (Huh7) are used in the liver constructs. The creation of aggregates of liver organoids and multipotent stromal cells derived from liver (LMSCs) are believed to increase the performance of the liver constructs as determined by hepatic function assays and gene-expression profiling. Bioreactors were custom designed and produced by stereolithography technology. Liver cells were printed in 5% w/v gelMA hydrogel and subsequently cross-linked by UV-A irradiation. The simultaneous deposition of pluronic F127 as a sacrificial support material allows the formation of a porous structure. After printing liver constructs are followed over time with cell viability assays including Alamar Blue and life-dead stainings. Cellular damage after treatment with toxic compounds is determined with an ATP assay.

Results: Cell aggregates remained viable for at least four days after 3D printing. The combination of liver organoids and LMSC aggregates in gelMA increased the albumin expression compared to single cell aggregates. However gene expression profiling of the single cell aggregates with only organoids showed a higher expression of early and late hepatic markers compared to the combined aggregates with organoids and LMSCs. No increased hepatic function of organoid and LMSC containing aggregates was observed with cytochrome P450 assays. As a control acute toxicity of the liver constructs was determined with a four-fold increase in ATP levels after Triton X-100 treatment at 2-3 days post printing. Placement of the porous liver construct in the custom designed bioreactor allowed the perfusion of the liver construct.

Conclusions: These results indicate that perfusable liver bioreactor systems have the potential to better predict DILI.



P2.3

Bioprinting of functional mouse thyroid gland organ construct

Hesuani Usef, Elena A Bulanova, Elizaveta Koudan, Aleksander Mitryashkin, Alexander Ostrovsky, Rodrigo Alvarenga Rezende, Frederico David Alencar Sena Pereira, Janaina de Andréa Dernowsek, Veronica Egidia Passamai, Jorge Vicente Lopes Silva, Vladimir Mironov
3D Bioprinting Solutions, Moscow, Russia

Aim: Organ printing is a main challenge of rapidly emerging 3D bioprinting technology. The bioprinted organ must be i) bioprinted according to specially developed digital model; ii) consist of authentic and histotypical structural-functional units of desirable organ; iii) well vascularized before implantation into recipient organism; iv) structurally integrated into single morphological entity; and most importantly v) demonstrate function in vivo on the level of organism. Our goal was to bioprint functional mouse thyroid gland construct which fits to these criteria for bioprinted organ.

Methods: The digital model of organ has been developed using open source computer-aided design software inVesalius (CTI Campinas Brazil). Embryonic explants of mouse thyroid (E14.5) gland have been dissected and rounded in hanging drops. It has been demonstrated using immunohistochemistry with specific endothelial marker (PECAM) and in vitro collagen angiogenesis assay that rounded embryonic thyroid explants (E8.5) are vascularized and contain around 1000 lumenized thyroid follicles. Lumenized vascular tissue spheroids have been biofabricated using hanging drop in the presence of vascular endothelial growth factor (VEGF) from isolated mouse allantoides. Original multifunctional 3D bioprinter Fabion (3D bioprinting Solutions Moscow Russia) has been used for bioprinting mouse thyroid gland construct according to digital model. The functional studies have been performed on animal model of thyroid gland hypofunction using radioactive iode-131. The level of thyroid hormone thyroxine (T4) in blood has been estimated in control mice after experimental thyroid hypofunction and after implantation of bioprinted thyroid tissue organ construct. The bioprinted mouse thyroid glands construct was also analyzed using standard morphological methods.

Results: Mouse thyroid gland has been bioprinted using rounded embryonic mouse thyroid gland explants and rounded mouse allantoies explants and collagen hydrogel. The functional studies demonstrated that bioprinted organ construct produce thyroid hormone thyroxine (T4) in the volume sufficient to compensate thyroid glands function loss in the radioactive animal model of thyroid gland hypofunction.

Conclusions: Our data demonstrated that the number of thyroid follicles the level of their maturation and vascularization in bioprinted mouse thyroid gland organ construct are sufficient to compensate lost function of thyroid glands in animal model of thyroid hypofunction. According our best knowledge it is a first report about successful 3D printing of functional mouse organ constructs. Thus we demonstrated that organ printing is an achievable goal. Our next logical step is 3D bioprinting of human thyroid gland construct using thyroid epithelium derived from human embryonic stem cells and/or human induced pluripotent stem cells.

